Characterizing a High-Level Waste Cold Cap via Elemental and Structural Configuration - 14185

Derek R Dixon*, Michael J Schweiger*, and Pavel Hrma*
*Pacific Northwest National Laboratory, Richland, WA 99354, derek.dixon@pnnl.gov

ABSTRACT

The process of converting high-level waste feed to an immobilized glass form takes place within a cold cap that covers a high-temperature (1150°C) glass melt in a Joule or induction-heated melter. Liquid slurry feed is continuously charged through the top of a melter. Within the cold cap, many glass forming reactions occur, and the glass-forming melt becomes connected. Gases trapped in the melt arrange into bubbles that create a layer of foam below the reacting feed and collapses into cavities. This foam layer thermally insulates the reacting feed and limits heat transfer from the molten glass below, thus affecting the rate of glass formation. Information about the glass formation is desired for use in a mathematical model designed to simulate melting in a cold cap. To explore this phenomenon, a set of high-level waste feed simulant samples were heat-treated at 5 K min^{-1} to temperatures ranging from 400°C to 1200°C for comparison with cold cap sections generated in a laboratory-scale melter. To estimate the temperature distribution in laboratory-produced cold caps, structural (i.e., bubble size and shape) and optical (i.e., color) features were compared with heat-treated samples using elemental maps and backscattered electron and optical micrographs. These results will be used to verify the recently developed mathematical model of the cold-cap.

INTRODUCTION

The Hanford Tank Waste Treatment and Immobilization Plant (WTP) is currently being constructed by Bechtel National, Inc., for the U.S. Department of Energy [1] to vitrify the high-level waste (HLW) portion of the nearly 200,000 m^3 of nuclear waste stored in underground tanks at the Hanford Site in southeastern Washington State [2]. While ~90% of the mass in the tanks is classified as low-activity waste (LAW), ~95% of the radioactivity is in the HLW fraction, making its disposal difficult [3]. The WTP will convert the waste into glass by charging the feed into a joule-heated ceramic melter [3]. During this process, a layer of reacting feed that is being converted to glass, known as a “cold cap”, forms on the top of the glass melt [4].

As the slurry feed is continuously charged into the melter, water evaporates, and the dry feed in the cold cap heats up while many reactions occur, including melting of salts, reactions between borates and salts, dissolution of quartz particles, and finally formation of the borosilicate glass melt [4]. Simultaneously, gases such as carbon monoxide, carbon dioxide, and nitrogen oxides are generated. In addition, oxygen is released from the oxidation-reduction reactions within the glass melt [5]. As those reactions proceed, the transient glass-forming melt becomes a connected liquid. Gas bubbles in the melt form a layer of foam below and within the cold cap and subsequently merge into larger gaseous cavities [4, 6]. Heat transfer into the reacting feed is restricted because of the insulating effect of the foam layer, which ultimately limits the rate of glass production [4].

For the design and verification of a mathematical model to simulate the melting in the cold cap, more information about the temperature distribution and the formation and behavior of the foam layer is needed. Such a mathematical model has been developed recently to simulate the melting of HLW and other waste feeds [4]. A set of experiments was designed to profile the cold-cap temperature for model verification.

Experimental cold caps were generated in the laboratory-scale melter (LSM) system [7, 8]. Fig. 1 shows a schematic of the LSM. To simulate heat transfer in a joule-heated melter, the LSM is arranged in a manner that the heat flows to the cold cap from the glass melt. In addition, the LSM allows the cold-cap configuration to be visually observed during charging and to be preserved through quenching for sectioning and further analysis [8]. This approach allows cold-cap sections to be compared with heat-treated samples, thus creating a link to the mathematical model. Extensive tests have been performed using HLW simulants to investigate operational issues, such as the effect of feeding rate on cold-cap formation [9].

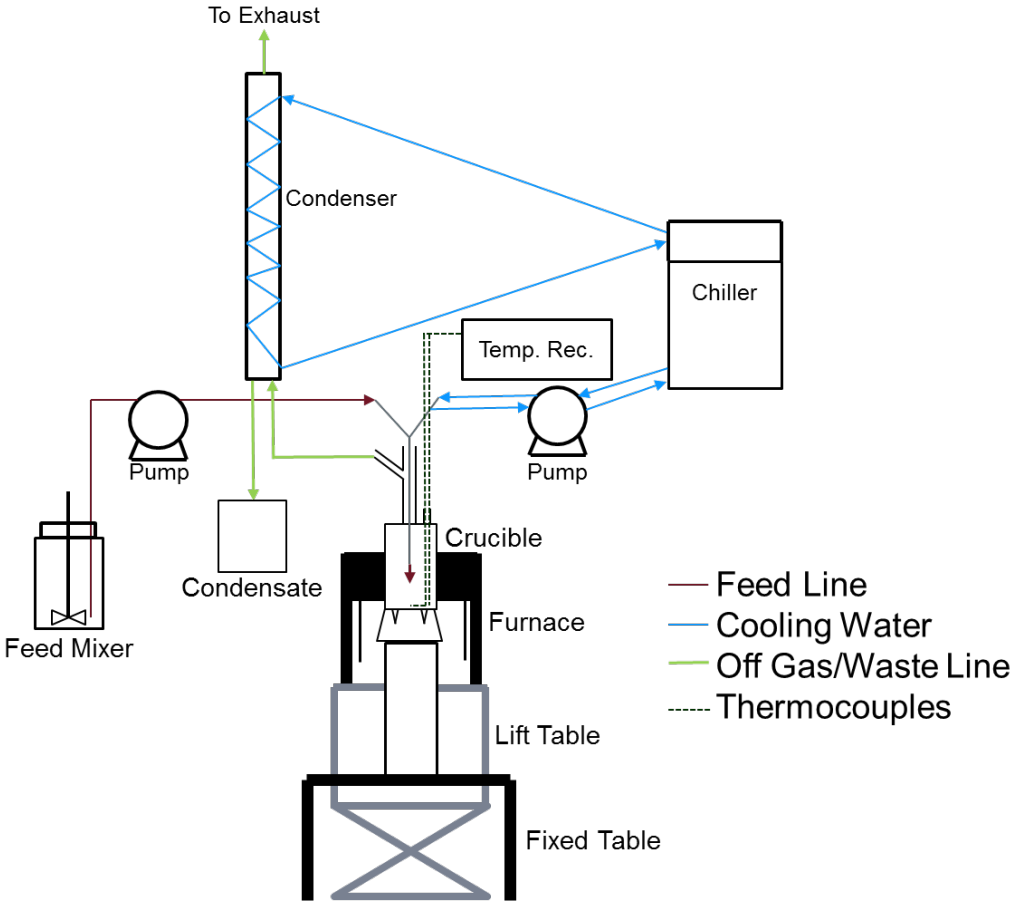

Fig. 1. Schematic of the LSM system. The pump on the left charges slurry feed into the crucible, and the pump on the right circulates cooling water from the chiller to the feed injection nozzle and back.

EXPERIMENTAL

Feed Composition and Preparation

A simulated high-alumina HLW feed, called A0, was used in these experiments (Table I [5, 9]). For each LSM test, a batch of 400 g glass L^{-1} A0 slurry was prepared by adding the components listed in Table I to ~800 mL of water using the same procedure as previously described [9].

Table I. Feed Composition and Component Mixing Order for 400g of A0 Glass

Compound	Amount (g)	Order Added
$Al(OH)_3$	146.99	7
$B(OH)_3$	107.93	5
$Bi(OH)_3$	5.12	4
CaO	24.31	4
$Fe(H_2PO_2)_3$	4.97	4
$Fe(OH)_3$	29.53	8
KNO_3	1.22	2
Li_2CO_3	35.32	6
$Mg(OH)_2$	0.68	4
$Na_2C_2O_4$	0.50	1
Na_2CrO_4	4.46	2
Na_2SO_4	1.42	1
NaF	5.91	4
$NaNO_2$	1.35	1
NaOH	39.77	3
$NiCO_3$	2.54	4
$Pb(NO_3)_2$	2.43	2
SiO_2	122.02	9
$Zn(NO_3)_2 \cdot 4H_2O$	1.06	1
$Zr(OH)_4 \cdot 0.65H_2O$	2.19	2
Total	539.74	-

LSM Setup and Operation

The LSM system (Fig. 1) was set up and operated as described in previous work [9] with the following changes:

- The amount of crushed A0 “initial” glass placed in the bottom of the fused-silica LSM crucible before melting was increased from 100 g to 200 g to prevent the cold, unreacted feed from reaching the bottom of the crucible during charging. This crushed glass melted in the furnace before feed charging began.
- A new Thermo Scientific ThermoFlex® 900[1] Chiller was used in the system to cool the off-gas condensation column and to provide 10°C water for the slurry injection nozzle.

Five LSM tests were performed. Each test was operated at a different feed charging rate (5.5, 6.5, 7.5, 8.5, and 9.5 mL min^{-1}). For the tests at 8.5 and 9.5 mL min^{-1}, the furnace had to be raised 5 and 10 mm, respectively, during the course of charging as converted feed increased the glass level. This ensured that the rising melt surface remained in the body of the furnace and did not reach the top shell of the furnace.

[1] ThermoFlex is a registered trademark of Thermo Scientific.

Heat Treatment of Slurry

Nine aliquots of the 400 g L^{-1} A0 slurry were transferred into separate ~1x1x1 cm^3 platinum crucibles. These slurry samples, initially weighing ~1 g, were placed in an oven at 105°C for 24 h. The batch was stirred at 30-min intervals until it thickened to a paste-like consistency and then left in the oven to dry. The mass of dried feed in each crucible weighed ~0.5 g. Each crucible was covered with platinum foil and placed on a raised platinum base in a furnace at room temperature. The furnace was heated at a rate of 5°C min^{-1} up to 1200°C, and starting at 400°C, one sample was removed at 100°C intervals.

RESULTS AND DISCUSSION

Examination of LSM Generated Cold Cap

The five LSM tests with 200-g initial glass were analyzed in the same way as the 100-g initial glass tests (charging rates 3.0, 4.0, 5.0, 6.0, 7.0 mL min^{-1}) performed previously [9]. The area (from a trace of the unreacted feed on the top view image of the glass melts [9]) and height (from the glass melt side view and cold-cap section images [9]) of the cold caps were measured using calibrated digital cameras and Adobe Photoshop[SM2] CS6 Extended software. Fig. 2 shows the results of both sets of tests where the height of the cold cap linearly increases with the charging rate. In addition, at the highest charging rate for each series of tests, the larger amount of the initial glass resulted in a smaller cold-cap area.

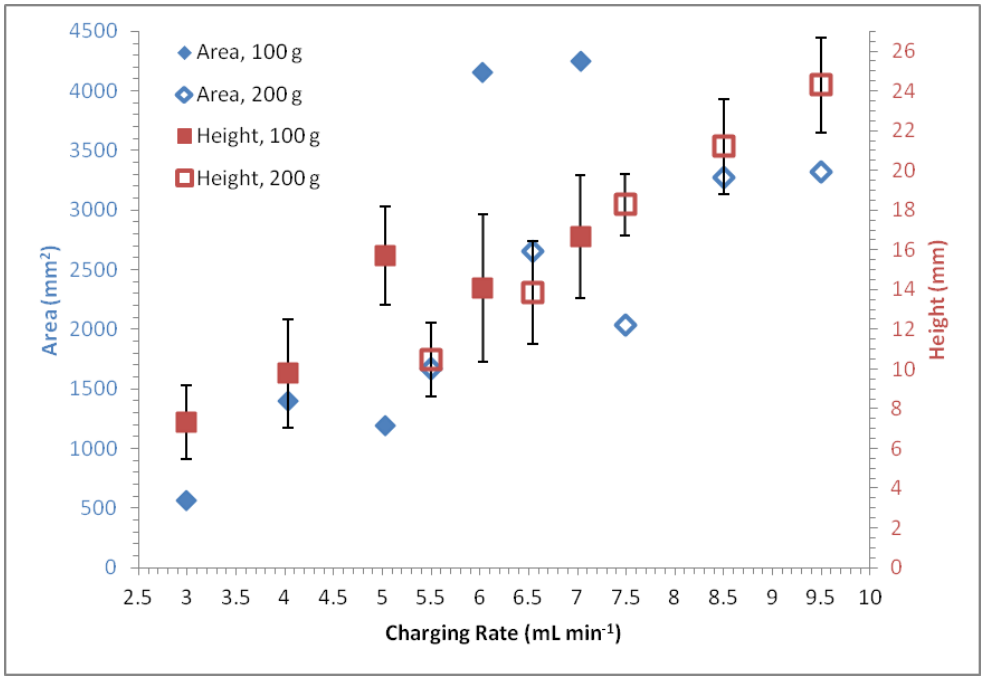

Fig. 2. Cold-cap height and area, prepared with 100- or 200-g initial glass, versus charging rate

After measuring the height and area, each cold cap was broken into sections to explore the internal structure of the cold cap. A section from the 6.5 mL min^{-1} test (Fig. 3) was mounted in epoxy, polished, and analyzed with scanning electron microscopy (SEM; JSM-7001F with a field

[2] Photoshop is a registered service mark of Adobe Systems Incorporated.

emission gun, JEOL, Ltd., Tokyo, Japan) and energy dispersive spectroscopy (EDS; EDAX Apollo II 30 mm2 silicon-drifted EDS detector, AMETEK, Berwyn, Pennsylvania). Specimens were analyzed both uncoated and coated with <1 nm of Au/Pd alloy. Both secondary electron and backscattered electron (BSE) detectors were used for imaging. Optical microscopy was performed with a Keyence VHX-2000E digital microscope, Fig. 3; the two regions marked were magnified for further analysis. The reacting feed, foam, and glass melt layer were investigated from this polished section.

Fig. 3. Polished cold-cap cross section from the 6.5 mL min^{-1} run. Regions for further analysis are marked by the blue (top of sample) and red boxes.

Heat-Treated Samples

A cross section of each heat-treated sample was mounted in epoxy and polished. Fig. 4 shows a matrix of optical images for the samples and lists their corresponding temperatures. The melt begins to connect at ~800°C as evolving gas is captured in bubbles and by 900°C is fully connected with many large bubbles. Bubbles are trapped in the feed at 800°C, but in the previous 700°C sample, evolved gasses vent through the porous cold cap.

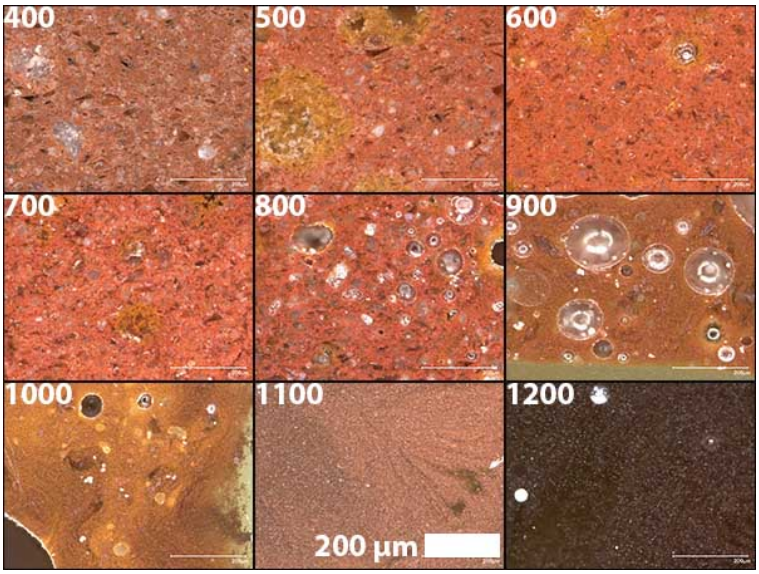

Fig. 4. Matrix of heat-treated samples of A0 composition. All temperatures are in units of °C, and all size bars denote 200 µm.

In addition to the polished cold-cap section (Fig. 3), the A0 samples heat-treated to 700°C, 800°C, and 900°C were analyzed with SEM. Fig. 5 compares SEM micrographs of the sample heat-treated to 900°C with that of the SEM and optical micrographs of the region marked by the red box (bottom of sample) on the cold-cap section. This region has similar characteristics to that of the 900°C sample including bubble size, silica particle size, and silica dissolution. As noted in the heat-treated samples (Fig. 4), the feed appears to be fully connected at 900°C, with bubbles ranging in size from 50 to 120 µm which is similar to features in the red box region of the cold cap (Fig. 3).

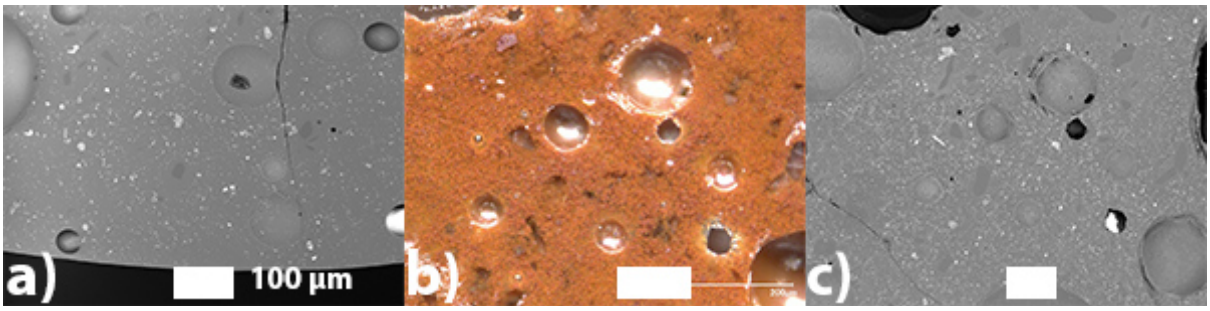

Fig. 5. a) BSE micrograph of heat-treated A0 feed at 900°C. A similarly structured region of the cold cap was found at the location of the marked red box in Fig. 3, as seen in images of an identical region from optical microscopy (image 5b) and BSE micrographs (5c).

The optical and BSE micrographs of A0 heat-treated samples at 700°C and 800°C shown in Fig. 6 show a difference in structure with respect to height within these samples. The melt is connected at the top of the samples; however, it remains unconnected at the bottom as noted by the epoxy voids appearing in black in the SEM micrograph. The thermal conductivity of the feed increases dramatically after ~800°C [10, 11] indicating that the heat transfer was limited prior to 800°C under these heat-treatment conditions (5°C min^{-1}) resulting in a gradient

temperature profile in these samples. Such gradient temperature profiles were not observed in the remaining heat-treated samples as shown in Fig. 4.

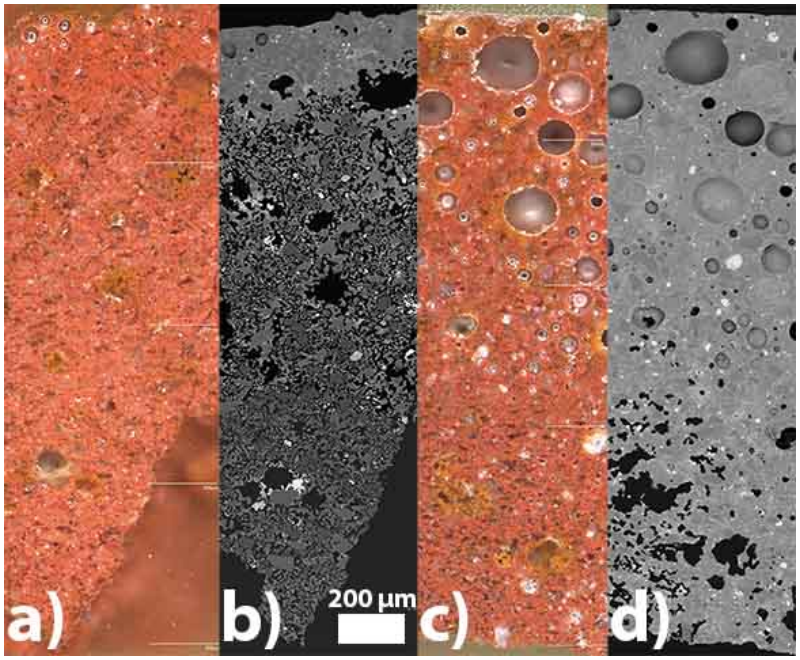

Fig. 6. Optical [a) and c)] and BSE [b) and d)] images of heat-treated A0 feed at 5 K min^{-1} to 700 [a) and b)] 800°C [c) and d)]

Energy Dispersive Spectroscopy Analysis

The cold-cap was further investigated with EDS by elemental mapping (Fig. 7) of the region denoted by the blue box in Fig. 3. Based on the reacting feed morphology, this region is similar to the 400°C sample shown in Fig. 4. The map revealed correlations between certain elements and particular structures observed in the electron and optical micrographs. For example, the yellow spots in the optical image mirror the bright white spots in the SEM image. The EDS analysis revealed that these spots are bismuth-rich regions as noted by the brightly colored spots in the 'Bi' map. In addition, regions rich in silicon, aluminum, iron, and calcium can be identified in the optical and SEM images based on their bright patterns from the EDS analysis. The large, milky white crystals in the optical image of the cold cap correspond with the dark grey regions in the SEM image. The EDS reveals that these crystals contain no silicon, aluminum, bismuth, calcium, or iron, while both boron and sodium are present. These crystals appear to be some form of a sodium borate mineral such as borax.

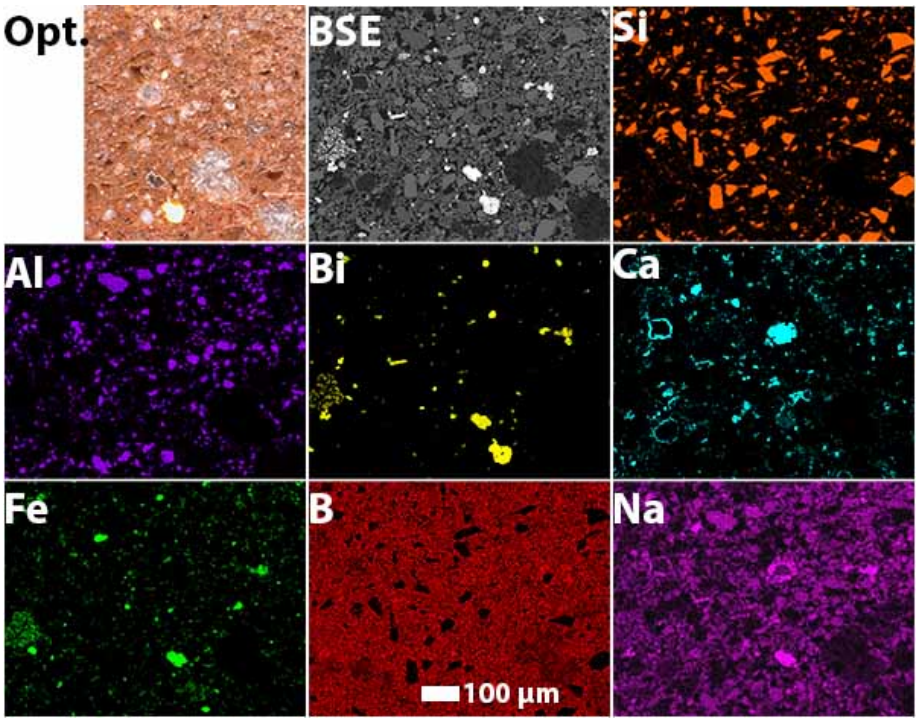

Fig. 7. Elemental map of a region near the top of the cold cap as shown by the blue box shown in Fig. 3

CONCLUSIONS

A series of tests created HLW cold caps at varying charging rates using the LSM system. The height of the cold cap increased linearly with increasing charging rate, while the area plateaued. The elemental and structural configuration within a cold cap was investigated by examining a cold-cap segment from the LSM test at 6.5 mL min^{-1} and feed samples heat-treated to specific temperatures. Thermal conductivity limitations caused a temperature gradient in samples heat-treated to 700°C and 800°C. Once the feed became fully connected (900°C), it was possible to identify equivalent temperature points within the cold cap and heat-treated samples. In addition, through EDS mapping, different structures, and spots in the cold cap could be related to specific elements, thereby helping to locate specific particles like bismuth and newly formed crystals such as borate. These correlations will be useful in the design and verification of the cold-cap mathematical model as the temperature gradient within the cold cap becomes better defined.

REFERENCES

1. BECHTEL NATIONAL INC, “About The Project,” http://www.hanfordvitplant.com/page/the-project/ (2013).
2. P. J. CERTA, P. A. EMPEY, M.N. WELLS, "River Protection Project System Plan," ORP-11242 Rev. 6, U.S. Department of Energy Office of River Protection, Richland, Washington,(2011).
3. A. A. KRUGER, "Advances in Glass Formulations for Hanford High-Aluminum, High-Iron and Enhanced Sulphate Management in HLW Streams," *WM2013 Conference*, Paper#13000, Phoenix, AZ (2013).
4. R. POKORNY, P. HRMA, "Mathematical modeling of cold cap," *Journal of Nuclear Materials*, **429**, 245-256 (2012).

5. D. A. PIERCE, P. HRMA, J. MARCIAL, B. J. RILEY, M. J. SCHWEIGER, "Effect of Alumina Source on the Rate of Melting Demonstrated with Nuclear Waste Glass Batch," *International Journal of Applied Glass Science*, **3**, 59-68 (2012).
6. R. POKORNY, P. HRMA, "Model for the conversion of nuclear waste melter feed to glass," *Journal of Nuclear Materials*, **445**, 190-199 (2014).
7. B. J. RILEY, J. V. CRUM, W. C. BUCHMILLER, B. T. RIECK, M. J. SCHWEIGER, J. D. VIENNA, "Initial Laboratory-Scale Melter Test Results for Combined Fission Product Waste," PNNL-18781, Pacific Northwest National Laboratory, Richland, WA, (2009).
8. D. S. KIM, M. J. SCHWEIGER, W. C. BUCHMILLER, J. MATYAS, "Laboratory-Scale Melter for Determination of Melting Rate of Waste Glass Feeds," PNNL-21005, Pacific Northwest National Laboratory, Richland, Washington, EMSP-RPT-012 (2012).
9. D. R. DIXON, M. J. SCHWEIGER, P. HRMA, "Effect of Feeding Rate on the Cold Cap Configuration in a Laboratory-Scale Melter," *WM2013 Conference*, Paper#13362, Phoenix, AZ (2013).
10. S. A. LOTTES, M. PETRICK, “Glass Furnace Model (GFM) Development and Technology Transfer Program,” ANL-07/28, Argonne National Laboratory, Argonne, IL (2007).
11. J. A. RICE, R. POKORNY, M. J. SCHWEIGER, P. HRMA, “Determination of heat conductivity and thermal diffusivity of waste glass melter feed: Extension to high temperatures,” In Preparation.

ACKNOWLEDGMENTS

This work was supported by the U.S. Department of Energy’s Waste Treatment and Immobilization Plant Federal Project Office under the direction of Dr. Albert A. Kruger. PNNL is operated for the Department of Energy by Battelle Memorial Institute under Contract DE-AC05-76RL0 1830. The authors would like to thank Shelley Carlson for mounting and polishing all samples for SEM work, and Brian Riley for his help operating the SEM/EDS instruments.